Design and Stabilization of Sampled-Data Neural-Network-Based Control Systems

H. K. Lam, *Member, IEEE*, and Frank H. F. Leung, *Senior Member, IEEE*

***Abstract*—This paper presents the design and stability analysis of a sampled-data neural-network-based control system. A continuous-time nonlinear plant and a sampled-data three-layer fully connected feedforward neural-network-based controller are connected in a closed loop to perform the control task. Stability conditions will be derived to guarantee the closed-loop system stability. Linear-matrix-inequality- and genetic-algorithm-based approaches will be employed to obtain the largest sampling period and the connection weights of the neural network subject to the considerations of the system stability and performance. An application example will be given to illustrate the design procedure and effectiveness of the proposed approach.**

***Index Terms*—Neural network, nonlinear system, sampled-data control.**

I. Introduction

THE SUPERIOR learning and generalization abilities of neural networks have attracted the public attention for many years. It was shown that a three-layer fully connected feedforward neural network (TLFCFFNN) is a universal approximator that is able to approximate any smooth continuous function in a compact domain to an arbitrary accuracy [1]. Owing to these outstanding properties, neural networks were widely applied in different applications to handle different problems such as forecasting [2], handwritten character recognition [3], automatic control [4], etc.

This paper focuses on the stability and the performance optimization issues of the neural-network-based sampled-data control systems. A neural-network-based control system is composed of a nonlinear plant and a neural-network-based controller connected in closed loop. The highly nonlinear nature of the plant and the neural network and the complexity of the network structure make the analysis difficult and complex. Different neural-network-based control approaches subject to the consideration of system stability were reported. In [5], an adaptive neural-network-based controller with variable hidden nodes was proposed. The stability of the closed-loop system is achieved by compensating the nonlinearity of the plant using the online estimated parameter values. The estimation error is a potential cause of the closed-loop system instability. To handle the effect of the estimation error to the system stability, adaptive neural-network-based controllers [6], [7] with switching control signals were proposed. However, the switching signals will introduce an undesired chattering effect to the system. In [8] and [9], adaptive neural networks combined with some conventional controllers were proposed. In most of these approaches, the use of the neural networks was mainly for modeling the nonlinearity of the plants. Other control schemes were then employed to achieve the system stability. In summary, the system stability was mostly achieved by the adaptive and/or sliding mode control techniques in these approaches, but not by the neural network itself. When the network parameters are online changing according to some adaptive laws, it will increase the computational demand, structural complexity, and implementation cost of the neural-network-based controller. In [10]–[12], stability conditions have been derived for a class of neural-network-based control systems with a feedforward multilayer-perceptron (MLP) neural network. The derived stability conditions were for checking the stability of the neural-network-based control systems. However, the ways for finding the network parameters and optimizing the system performance were ignored. These are in fact two important issues for putting the neural-network-based controller into practice.

In most of the published work, the investigations were based on purely continuous-time or discrete-time neural-network-based control systems; the sampled-data neural-network-based control systems are seldom considered. To investigate the system stability, the sampled-data systems can be regarded as systems with time-varying delays [13]–[16]. In this paper, sampled-data TLFCFFNN-based control systems subject to parameter uncertainties will be studied. The nonlinearity of the plant needs to be considered during the design of the sampled-data TLFCFFNN-based controller. Furthermore, the control signals are kept constant during the sampling period and cannot be changed to deal with the nonlinearity of the plant. These characteristics make the analysis and design more difficult and complex. In this paper, stability conditions will be derived to guarantee the stability of the sampled-data TLFCFFNN-based control systems using the Lyapunov-based approach. The finding of the largest sampling period and the connection weights of the TLFCFFNN-based controllers and the optimization of the system performance subject to the system stability will be formulated as a generalized eigenvalue minimization problem (GEVP) [17] and a genetic algorithm (GA) [18] minimization problem, respectively.

Manuscript received January 13, 2005; revised May 2, 2005, September 1, 2005, and October 26, 2005. This work was supported by the Hong Kong Polytechnic University under Grant G-YX31. This paper was recommended by Associate Editor W. J. Wang.

H. K. Lam is with the Department of Electronic Engineering, Division of Engineering, King's College London, London WC2R 2LS, U.K.

F. H. F. Leung is with the Centre for Multimedia Signal Processing, Department of Electronic and Information Engineering, Hong Kong Polytechnic University, Kowloon, Hong Kong.

Digital Object Identifier 10.1109/TSMCB.2006.872262

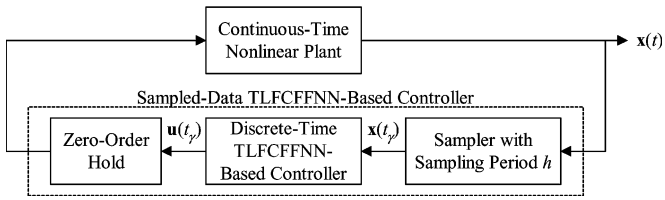

Fig. 1. Block diagram of a TLFCFFNN-based control system.

II. Nonlinear System and Neural-Network-Based Controller

A TLFCFFNN-based control system as shown in Fig. 1 consists of a continuous-time nonlinear system and a TLFCFFNN-based controller. Referring to this figure, the sampled-data TLFCFFNN-based controller is formed by a sampler with sampling period h, a discrete-time TLFCFFNN-based controller, and a zero-order-hold (ZOH) unit. With this control framework, the development and implementation costs may be reduced as the sampled-data TLFCFFNN-based controller can easily be realized by a microcomputer.

A. Nonlinear Plant

The continuous-time nonlinear plant to be controlled is of the following form:

$$\dot{\mathbf{x}}(t) = \mathbf{f}\left(\mathbf{x}(t), \mathbf{u}(t)\right) \tag{1}$$

where $\mathbf{x}(t) = [x_1(t)\ x_2(t)\ \cdots\ x_n(t)]^{\mathrm{T}} \in \Re^{n\times 1}$ is the system state vector; $\mathbf{u}(t) = [u_1(t)\ u_2(t)\ \cdots\ u_m(t)]^{\mathrm{T}} \in \Re^{m\times 1}$ is the input vector; and $\mathbf{f}(\cdot)$ denotes a nonlinear function with known form. The nonlinear plant of (1) can be written in the following form [22], [23]:

$$\dot{\mathbf{x}}(t) = \sum_{i=1}^{p} w_i\left(\mathbf{x}(t)\right)\left(\mathbf{A}_i\mathbf{x}(t) + \mathbf{B}_i\mathbf{u}(t)\right) \tag{2}$$

where $\mathbf{A}_i \in \Re^{n\times n}$ and $\mathbf{B}_i \in \Re^{n\times m}$ are the constant system and input matrices, respectively; p is a nonzero positive integer; and $w_i(\mathbf{x}(t))$ has the following properties:

$$\sum_{i=1}^{p} w_i\left(\mathbf{x}(t)\right) = 1, \qquad w_i\left(\mathbf{x}(t)\right) \in [0\ 1]; \quad i = 1, 2, \ldots, p. \tag{3}$$

Remark 1: Based on the assumption that the nonlinear plant can be represented in the general form of (1), there are two ways to obtain the system model in the form of (2) for the nonlinear plant, namely: 1) by system identification techniques [22] based on the input–output data and 2) by mathematical derivation [23] if the nonlinear plant can be represented as $\dot{\mathbf{x}}(t) = \mathbf{A}(\mathbf{x}(t))\mathbf{x}(t) + \mathbf{B}(\mathbf{x}(t))\mathbf{u}(t)$, where $\mathbf{A}(\mathbf{x}(t))$ and $\mathbf{B}(\mathbf{x}(t))$ are the system and input matrices of the nonlinear plant, respectively. It is assumed in the second method that the form of the mathematical model is known. Notice that the value of $w_i(\mathbf{x}(t))$ is unknown if the nonlinear plant is subject to parameter uncertainties.

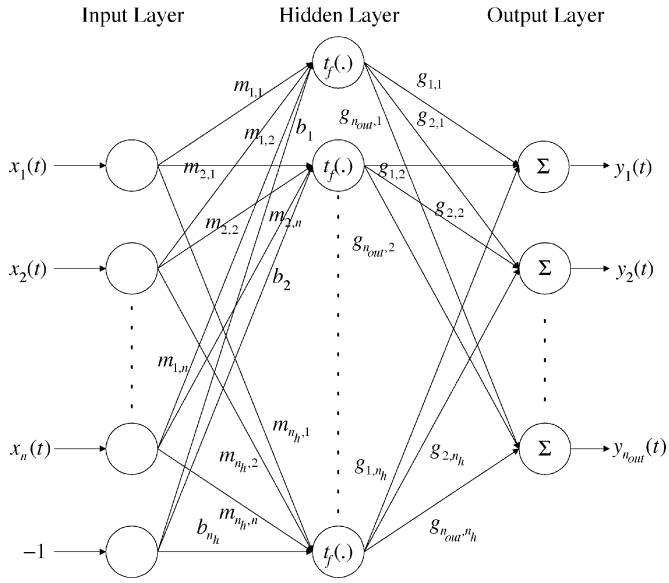

Fig. 2. TLFCFFNN.

B. Sampled-Data Three-Layer Fully Connected Feedforward Neural-Network-Based Controller

A traditional multiple-input-multiple-output discrete-time TLFCFFNN [19] is shown in Fig. 2. Its input–output relationship is given by

$$y_k(t_\gamma) = \sum_{j=1}^{n_h} g_{k,j} t_f\left(\sum_{i=1}^{n} m_{j,i} x_i(t_\gamma) - b_j\right), \qquad k = 1, 2, \ldots, n_{\mathrm{out}} \tag{4}$$

where $t_\gamma = \gamma h,\ \gamma = 0, 1, 2, \ldots, \infty$, denotes a time instant; $h = t_{\gamma+1} - t_\gamma$ denotes the constant sampling period; $m_{j,i}$ denotes the connection weight between the jth hidden node and the ith input node; $g_{k,j}$ denotes the connection weight between the kth output node and the jth hidden node; b_j denotes the bias for the jth hidden node; $t_f(\cdot)$ denotes the activation function; n_h denotes the number of hidden nodes; n_{out} denotes the number of output nodes; $\mathbf{x}(t_\gamma) = [x_1(t_\gamma)\ x_2(t_\gamma)\ \cdots\ x_n(t_\gamma)]^{\mathrm{T}}$ denotes the sampled system state vector at time instant t_γ. The sampled-data TLFCFFNN-based controller for the nonlinear system of (2), with $n_{\mathrm{out}} = mn$, is defined as $\mathbf{u}(t)$, as in (5) shown at the bottom of the next page.

It should be noted that $\mathbf{u}(t) = \mathbf{u}(t_\gamma)$, which holds constant value by the ZOH unit during $t_\gamma < t \le t_{\gamma+1}$. From (4) and (5), we have

$$\mathbf{u}(t) = \sum_{j=1}^{n_h} m_j\left(\mathbf{x}(t_\gamma)\right)\mathbf{G}_j\mathbf{x}(t_\gamma), \qquad \gamma = 0, 1, 2, \ldots, \infty \tag{6}$$

where

$$\mathbf{G}_j = \begin{bmatrix} g_{1,j} & g_{2,j} & \cdots & g_{n,j} \\ g_{n+1,j} & g_{n+2,j} & \cdots & g_{2n,j} \\ \vdots & \vdots & \ddots & \vdots \\ g_{(m-1)n+1,j} & g_{(m-1)n+2,j} & \cdots & g_{mn,j} \end{bmatrix} \quad (7)$$

$$m_j\left(\mathbf{x}(t_\gamma)\right) = \frac{t_f\left(\sum_{i=1}^{n} m_{j,i}x_i(t_\gamma) - b_j\right)}{\sum_{l=1}^{n_h} t_f\left(\sum_{v=1}^{n} m_{l,v}x_v(t_\gamma) - b_l\right)} \in [0\ 1] \quad (8)$$

which exhibits the property that $\sum_{j=1}^{n_h} m_j(\mathbf{x}(t_\gamma)) = 1$. The activation function $t_f(\cdot)$ is chosen such that $t_f(\sum_{v=1}^{n} m_{l,v}x_v(t_\gamma) - b_l) \geq 0$ for all $l = 1, 2, \ldots, n_h$, and $\sum_{l=1}^{n_h} t_f(\sum_{v=1}^{n} m_{l,v}x_v(t_\gamma) - b_l) \neq 0$ at any time so as to satisfy the property of (8).

Remark 2: Referring to (2), the dynamical behavior of the nonlinear plant is characterized by $w_i(\mathbf{x}(t))$, $\mathbf{A}_i$, and $\mathbf{B}_i$. A sampled-data TLFCFFNN-based controller is proposed to stabilize the nonlinear plant. As the control action of the sampled-data TLFCFFNN-based controller is mainly governed by the parameters of the neural network, i.e., $m_{j,i}$ and $g_{k,j}$, its stabilizability is governed by the network parameters. In the following sections, the design of the network parameters based on the nonlinear plant's parameters will be formulated as a linear-matrix inequality (LMI) problem under the consideration of system stability. It will be shown later on that the network parameter $g_{k,j}$ mainly determines the system stability. Their values will be designed based on the nonlinear plant's parameters $\mathbf{A}_i$ and $\mathbf{B}_i$. The network parameter $m_{j,i}$, on the other hand, only affects the closed-loop system performance. Their values will be determined using GA to optimize the system performance.

C. Sampled-Data TLFCFFNN-Based Control Systems

A sampled-data TLFCFFNN-based control system as shown in Fig. 1 is formed by connecting the continuous-time nonlinear system of (2) and the sampled-data TLFCFFNN-based controller of (6) in closed loop. In the following, $w_i(\mathbf{x}(t))$ and $m_j(\mathbf{x}(t_\gamma))$ are written as w_i and m_j, respectively, for simplicity. Let $\tau(t) = t - t_\gamma \leq h$ for $t_\gamma < t \leq t_{\gamma+1}$, from (2) and (6) and the property that $\sum_{i=1}^{p} w_i = \sum_{j=1}^{n_h} m_j = \sum_{i=1}^{p}\sum_{j=1}^{n_h} w_i m_j = 1$, we have

$$\dot{\mathbf{x}}(t) = \sum_{i=1}^{p}\sum_{j=1}^{n_h} w_i m_j \left(\mathbf{A}_i\mathbf{x}(t) + \mathbf{B}_i\mathbf{G}_j\mathbf{x}\left(t - \tau(t)\right)\right). \quad (9)$$

III. Stability and Design of Sampled-Data TLFCFFNN-Based Control Systems

The stability, design, and performance optimization of the sampled-data TLFCFFNN-based control system of (9) will be investigated in this section.

A. Stability Analysis and Maximum Sampling Period

The solution to 1) the stability conditions in terms of LMIs [17], 2) the connection weights of the TLFCFFNN, and 3) the maximum sampling period can be determined by solving the GEVP stated in the following theorem.

Theorem 1: The sampled-data TLFCFFNN-based control system of (9) formed by the continuous-time nonlinear system in the form of (2) and the sampled-data TLFCFFNN-based controller of (6) is guaranteed to be asymptotically stable if there exist matrices $\mathbf{X}_1 \in \Re^{n\times n}$, $\mathbf{X}_2 \in \Re^{n\times n}$, $\mathbf{X}_3 \in \Re^{n\times n}$, $\mathbf{M} \in \Re^{n\times n}$, $\mathbf{M}_{ij}^{(11)} \in \Re^{n\times n}$, $\mathbf{M}_{ij}^{(21)} \in \Re^{n\times n}$, $\mathbf{M}_{ij}^{(22)} \in \Re^{n\times n}$, $\mathbf{Y} \in \Re^{n\times n}$, and $\mathbf{N}_j \in \Re^{m\times n}$, $i = 1, 2, \ldots, p$; $j = 1, 2, \ldots, n_h$, such that the LMIs given at the bottom of the page are satisfied,

$$\mathbf{u}(t) = \frac{\begin{bmatrix} y_1(t_\gamma) & y_2(t_\gamma) & \cdots & y_n(t_\gamma) \\ y_{n+1}(t_\gamma) & y_{n+2}(t_\gamma) & \cdots & y_{2n}(t_\gamma) \\ \vdots & \vdots & \ddots & \vdots \\ y_{(m-1)n+1}(t_\gamma) & y_{(m-1)n+2}(t_\gamma) & \cdots & y_{mn}(t_\gamma) \end{bmatrix} \begin{bmatrix} x_1(t_\gamma) \\ x_2(t_\gamma) \\ \vdots \\ x_n(t_\gamma) \end{bmatrix}}{\sum_{l=1}^{n_h} t_f\left(\sum_{v=1}^{n} m_{l,v}x_v(t_\gamma) - b_l\right)}, \qquad t_\gamma < t \leq t_{\gamma+1} \quad (5)$$

$$\mathbf{X}_1 = \mathbf{X}_1^{\mathrm{T}} > 0, \quad \mathbf{M} = \mathbf{M}^{\mathrm{T}} > 0, \quad \mathbf{Y} = \mathbf{Y}^{\mathrm{T}} > 0, \quad \begin{bmatrix} 2\mathbf{X}_1 - \mathbf{M} & \mathbf{0} & \mathbf{N}_j^{\mathrm{T}}\mathbf{B}_i^{\mathrm{T}} \\ \mathbf{0} & \mathbf{M}_{ij}^{(11)} & \mathbf{M}_{ij}^{(21)^{\mathrm{T}}} \\ \mathbf{B}_i\mathbf{N}_j & \mathbf{M}_{ij}^{(21)} & \mathbf{M}_{ij}^{(22)} \end{bmatrix} \geq 0$$

$$\begin{bmatrix} \mathbf{M}_{ij}^{(11)} & \mathbf{M}_{ij}^{(21)^{\mathrm{T}}} & \mathbf{X}_1 & \mathbf{X}_2^{\mathrm{T}} \\ \mathbf{M}_{ij}^{(21)} & \mathbf{M}_{ij}^{(22)} & \mathbf{0} & \mathbf{X}_3^{\mathrm{T}} \\ \mathbf{X}_1 & \mathbf{0} & -\mathbf{Y} & \mathbf{0} \\ \mathbf{X}_2 & \mathbf{X}_3 & \mathbf{0} & -\mathbf{M} \end{bmatrix} < -\frac{1}{h}\begin{bmatrix} \mathbf{X}_2 + \mathbf{X}_2^{\mathrm{T}} & \mathbf{X}_1\mathbf{A}_i^{\mathrm{T}} + \mathbf{N}_j^{\mathrm{T}}\mathbf{B}_i^{\mathrm{T}} - \mathbf{X}_2^{\mathrm{T}} + \mathbf{X}_3 & \mathbf{0} & \mathbf{0} \\ \mathbf{A}_i\mathbf{X}_1 + \mathbf{B}_i\mathbf{N}_j - \mathbf{X}_2 + \mathbf{X}_3^{\mathrm{T}} & -\mathbf{X}_3 - \mathbf{X}_3^{\mathrm{T}} & \mathbf{0} & \mathbf{0} \\ \mathbf{0} & \mathbf{0} & \mathbf{0} & \mathbf{0} \\ \mathbf{0} & \mathbf{0} & \mathbf{0} & \mathbf{0} \end{bmatrix}$$

for $i = 1, 2, \ldots, p;\ j = 1, 2, \ldots, n_h$, where the connection weights of the TLFCFFNN are defined as $\mathbf{G}_j = \mathbf{N}_j \mathbf{X}_1^{-1}$.

The largest sampling period h is obtained by solving the following GEVP:

$$\underset{\mathbf{X}_1, \mathbf{X}_2, \mathbf{X}_3, \mathbf{M}_{ij}^{(11)}, \mathbf{M}_{ij}^{(21)}, \mathbf{M}_{ij}^{(22)}, \mathbf{M}, \mathbf{Y}, \mathbf{N}_j}{\text{minimize}} \frac{1}{h}$$

subject to the above LMIs.

Proof: The proof is given in Appendix A. ■

Remark 3: The largest value of h denotes the largest sampling period that the sampled-data TLFCFFNN-based controller is guaranteed to stabilize the nonlinear system.

Remark 4: It can be seen from Theorem 1 that the stability conditions do not involve the plant parameter w_i. In other words, the value of w_i does not affect the system stability, which enhances the robustness of the closed-loop system if the parameter uncertainties of the nonlinear plant are only affecting w_i.

Remark 5: It can be seen from Theorem 1 that the stability conditions depend only on the network parameter $g_{k,j}$ (element of $\mathbf{G}_j = \mathbf{N}_j \mathbf{X}_1^{-1}$) and not on the network parameter $m_{j,i}$. By solving the stability conditions in Theorem 1, the value of $g_{k,j}$ can be obtained. Furthermore, the values of $m_{j,i}$ can be freely designed to achieve good system performance, as long as the constraints $t_f(\sum_{v=1}^{n} m_{l,v} x_v(t_\gamma) - b_l) \geq 0$ and $\sum_{l=1}^{n_h} t_f(\sum_{v=1}^{n} m_{l,v} x_v(t_\gamma) - b_l) \neq 0$ are satisfied.

B. Performance Optimization

The maximum sampling period $h_{\max}$ can be obtained by using Theorem 1. A sampling period h between 0 and $h_{\max}$, i.e., $0 < h \leq h_{\max}$, can be employed as the sampling period of the sampled-data TLFCFFNN-based controller. Under this chosen h, the stability of the sampled-data TLFCFFNN-based control system is guaranteed by Theorem 1. In the following, the system performance will then be optimized based on the LMI approach under the chosen constant sampling period h. The performance of a system can be quantitatively measured by the following performance index, which is commonly used in optimal control [20].

$$J = \int_{\tau_0}^{\tau_1} \begin{bmatrix} \mathbf{x}(t_\gamma) \\ \mathbf{u}(t) \end{bmatrix}^{\mathrm{T}} \begin{bmatrix} \mathbf{J}_1 & \mathbf{J}_2 \\ \mathbf{J}_2^{\mathrm{T}} & \mathbf{J}_3 \end{bmatrix} \begin{bmatrix} \mathbf{x}(t_\gamma) \\ \mathbf{u}(t) \end{bmatrix} dt_\gamma \tag{10}$$

where $\tau_1 - \tau_0 > 0$ denote the optimization period, $\mathbf{J}_1 = \mathbf{J}_1^{\mathrm{T}} > 0$, $\mathbf{J}_3 = \mathbf{J}_3^{\mathrm{T}} > 0$, and $\begin{bmatrix} \mathbf{J}_1 & \mathbf{J}_2 \\ \mathbf{J}_2^{\mathrm{T}} & \mathbf{J}_3 \end{bmatrix} > 0$, which is determined by the designer. The performance optimization can be formulated as a GEVP and summarized into the following theorem.

Theorem 2: The sampled-data TLFCFFNN-based system of (9) formed by the continuous-time nonlinear system in the form of (2) and the sampled-data TLFCFFNN-based controller of (6) is guaranteed to be asymptotically stable if there exist matrices $\mathbf{X}_1 \in \Re^{n\times n}$, $\mathbf{X}_2 \in \Re^{n\times n}$, $\mathbf{X}_3 \in \Re^{n\times n}$, $\mathbf{M} \in \Re^{n\times n}$, $\mathbf{M}_{ij}^{(11)} \in \Re^{n\times n}$, $\mathbf{M}_{ij}^{(21)} \in \Re^{n\times n}$, $\mathbf{M}_{ij}^{(22)} \in \Re^{n\times n}$, $\mathbf{Y} \in \Re^{n\times n}$, and $\mathbf{N}_j \in \Re^{m\times n}$, $i = 1, 2, \ldots, p;\ j = 1, 2, \ldots, n_h$, such that the LMIs given at the bottom of the page are satisfied, with a defined constant sampling period $0 \leq h \leq h_{\max}$: for $i = 1, 2, \ldots, p;\ j = 1, 2, \ldots, n_h$, where the connection weights of the TLFCFFNN are defined as $\mathbf{G}_j = \mathbf{N}_j \mathbf{X}_1^{-1}$.

The system performance of (10) is optimized by solving the following GEVP:

$$\underset{\mathbf{X}_1, \mathbf{X}_2, \mathbf{X}_3, \mathbf{M}_{ij}^{(11)}, \mathbf{M}_{ij}^{(21)}, \mathbf{M}_{ij}^{(22)}, \mathbf{M}, \mathbf{Y}, \mathbf{N}_j}{\text{minimize}} \eta$$

subject to the above LMIs.

Proof: The proof is given in Appendix B. ■

Remark 6: A constant value should be assigned to h ($0 < h \leq h_{\max}$) before applying Theorem 2, where the maximum sampling period $h_{\max}$ is obtained by Theorem 1.

Remark 7: It should be noted that $\mathbf{J}_1 \in \Re^{n\times n}$ and $\mathbf{J}_3 \in \Re^{m\times m}$ are constant symmetric matrices and $\mathbf{J}_2 \in \Re^{n\times m}$ is a constant arbitrary matrix. Their values must be determined before applying Theorem 2.

C. Tuning of $m_{j,i}$ and b_j

In Theorems 1 and 2, the maximum sampling period and the connection weight $g_{k,j}$ are determined based on the LMI approach. In this section, the connection weight $m_{j,i}$ and the

$$\mathbf{X}_1 = \mathbf{X}_1^{\mathrm{T}} > 0, \quad \mathbf{M} = \mathbf{M}^{\mathrm{T}} > 0, \quad \mathbf{Y} = \mathbf{Y}^{\mathrm{T}} > 0, \quad \begin{bmatrix} 2\mathbf{X}_1 - \mathbf{M} & \mathbf{0} & \mathbf{N}_j^{\mathrm{T}} \mathbf{B}_i^{\mathrm{T}} \\ \mathbf{0} & \mathbf{M}_{ij}^{(11)} & \mathbf{M}_{ij}^{(21)^{\mathrm{T}}} \\ \mathbf{B}_i \mathbf{N}_j & \mathbf{M}_{ij}^{(21)} & \mathbf{M}_{ij}^{(22)} \end{bmatrix} \geq 0$$

$$\begin{bmatrix} \mathbf{X}_2 + \mathbf{X}_2^{\mathrm{T}} + h\mathbf{M}_{ij}^{(11)} & \mathbf{X}_1 \mathbf{A}_i^{\mathrm{T}} + \mathbf{N}_j^{\mathrm{T}} \mathbf{B}_i^{\mathrm{T}} - \mathbf{X}_2^{\mathrm{T}} + \mathbf{X}_3 + h\mathbf{M}_{ij}^{(21)^{\mathrm{T}}} & h\mathbf{X}_1 & h\mathbf{X}_2^{\mathrm{T}} \\ \mathbf{A}_i \mathbf{X}_1 + \mathbf{B}_i \mathbf{N}_j - \mathbf{X}_2 + \mathbf{X}_3^{\mathrm{T}} + h\mathbf{M}_{ij}^{(21)} & -\mathbf{X}_3 - \mathbf{X}_3^{\mathrm{T}} + h\mathbf{M}_{ij}^{(22)} & \mathbf{0} & h\mathbf{X}_3^{\mathrm{T}} \\ h\mathbf{X}_1 & \mathbf{0} & -h\mathbf{Y} & \mathbf{0} \\ h\mathbf{X}_2 & h\mathbf{X}_3 & \mathbf{0} & -h\mathbf{M} \end{bmatrix} < 0$$

$$\begin{bmatrix} \mathbf{J}_1 & \mathbf{J}_2 \\ \mathbf{J}_2^{\mathrm{T}} & \mathbf{J}_3 \end{bmatrix} > 0, \quad \begin{bmatrix} -\eta\mathbf{I} & \mathbf{X}_1 & \mathbf{N}_j^{\mathrm{T}} \\ \mathbf{X}_1 & -\begin{bmatrix} \mathbf{J}_1 & \mathbf{J}_2 \\ \mathbf{J}_2^{\mathrm{T}} & \mathbf{J}_3 \end{bmatrix}^{-1} & \\ \mathbf{N}_j & & \end{bmatrix} < 0$$

bias b_j will be determined. Owing to the nonlinear nature of the activation function of the TLFCFFNN, it is difficult to formulate the finding of $m_{j,i}$ and b_j into an LMI problem. Instead, GA can be employed to tune the values of $m_{j,i}$ and b_j by minimizing the following performance index for the closed-loop system:

$$J = \int_{\tau_0}^{\tau_1} \begin{bmatrix} \mathbf{x}(t) \\ \mathbf{u}(t) \end{bmatrix}^{\mathrm{T}} \begin{bmatrix} \mathbf{J}_1 & \mathbf{J}_2 \\ \mathbf{J}_2^{\mathrm{T}} & \mathbf{J}_3 \end{bmatrix} \begin{bmatrix} \mathbf{x}(t) \\ \mathbf{u}(t) \end{bmatrix} dt. \tag{11}$$

It should be noted that the values of the sampling period h and the connection weight $g_{k,j}$ obtained by Theorem 1 or 2 are kept constant during the training process. As the system stability is governed by the sampling period and the connection weight $g_{k,j}$ only, the values of $m_{j,i}$ and b_j can be freely tuned to alter the system performance.

D. Design Procedure

The design procedure of the sampled-data TLFCFFNN-based controller is given as follows.

Step 1) Obtain the model of the nonlinear plant in the form of (2).

Step 2) Determine the number of hidden node n_h and the activation functions for the sampled-data TLFCFFNN-based controller in the form of (6).

Step 3) Determine the maximum sampling period $h_{\max}$ by Theorem 1. Choose a constant sampling period h such that $0 < h \leq h_{\max}$.

Step 4) Under the chosen sampling period h in Step 3), optimize the system performance and obtain the connection weight $g_{k,j}$ based on Theorem 2.

Step 5) Under the chosen sampling period h and the connection weight $g_{k,j}$, obtain the connection weight $m_{j,i}$ and the bias b_j by the GA process.

Step 6) Realize the sampled-data TLFCFFNN-based controller based on the determined values of h, $g_{k,j}$, $m_{j,i}$, and b_j.

IV. Application Example

The proposed sampled-data TLFCFFNN-based controller will be employed to stabilize an inverted pendulum subject to parameter uncertainties. The objective is to drive the system state of the inverted pendulum to zero at the steady state.

Step 1) The system behaviour of the inverted pendulum is described by the following dynamic equation.

$$\ddot{\theta}(t) = \frac{g \sin(\theta(t)) - am_p L\dot{\theta}(t)^2 \frac{\sin(2\theta(t))}{2} - a\cos(\theta(t))\, u(t)}{\frac{4L}{3} - am_p L\cos^2(\theta(t))} \tag{12}$$

where $\theta(t)$ is the angular displacement of the pendulum, $g = 9.8\ \mathrm{m/s^2}$ is the acceleration due to gravity, $m_p \in [m_{p_{\min}}\ m_{p_{\max}}] = [2\ 5]$ kg is the mass of the pendulum, $M_c \in [M_{c_{\min}}\ M_{c_{\max}}] = [30\ 35]$ kg is the mass of the cart, $a = 1/(m_p + M_c)$, $2L = 1$ m is the length of the pendulum, and $u(t)$ is the force applied to the cart, m_p and M_c are regarded as the parameter uncertainties. The inverted pendulum subject to parameter uncertainties can be represented by the following model:

$$\dot{\mathbf{x}}(t) = \sum_{i=1}^{4} w_i(\mathbf{x}(t))\left(\mathbf{A}_i\mathbf{x}(t) + \mathbf{B}_i u(t)\right) \tag{13}$$

where $\mathbf{x}(t) = [x_1(t)\ x_2(t)]^{\mathrm{T}} = [\theta(t)\ \dot{\theta}(t)]^{\mathrm{T}}$, $x_1(t) \in [x_{1_{\min}}\ \ x_{1_{\max}}] = [-\pi/3\ \ \pi/3]$, and $x_2(t) \in [x_{2_{\min}}\ \ x_{2_{\max}}] = [-5\ \ 5]$. The parameters of the model are listed in Appendix C.

Step 2) A sampled-data TLFCFFNN-based controller with four hidden nodes is employed to control the inverted pendulum. From (6), the sampled-data TLFCFFNN-based controller is given by

$$u(t) = \sum_{j=1}^{4} m_j(\mathbf{x}(t_\gamma))\,\mathbf{G}_j\mathbf{x}(t_\gamma), \quad t_\gamma < t \leq t_{\gamma+1}, \quad \gamma = 0, 1, 2, \ldots, \infty. \tag{14}$$

The logarithmic sigmoid function is used as the transfer function, i.e., $t_f(\sum_{i=1}^{2} m_{j,i}x_i(t_\gamma) - b_j) = 1/(1 + \exp[-(\sum_{i=1}^{2} m_{j,i}x_i(t_\gamma) - b_j)])$.

Step 3) The largest sampling period $h_{\max}$ is found to be 0.0662 s based on Theorem 1. A constant sampling period $0 < h = 0.05 < h_{\max}$ is chosen for the sampled-data TLFCFFNN-based controller.

Step 4) The performance index of (10) will be optimized to achieve the system performance. We choose $\mathbf{J}_1 = \begin{bmatrix} 10 & 0 \\ 0 & 1 \end{bmatrix}$, $\mathbf{J}_2 = \begin{bmatrix} 0 \\ 0 \end{bmatrix}$, and $\mathbf{J}_3 = 0.01$ in this application example. The MATLAB LMI toolbox is employed to solve the solution of the GEVP in Theorem 2. The connection weights $\mathbf{G}_j = \mathbf{N}_j\mathbf{X}_1^{-1}$ are shown in Table I.

TABLE I
VALUES OF THE CONNECTION WEIGHT $g_{k,j}$ WITH $\mathbf{J}_2 = \begin{bmatrix} 0 \\ 0 \end{bmatrix}$ AND $\mathbf{J}_3 = 0.01$

Connection Weights	$\mathbf{J}_1 = \begin{bmatrix} 10 & 0 \\ 0 & 1 \end{bmatrix}$	$\mathbf{J}_1 = \begin{bmatrix} 100 & 0 \\ 0 & 1 \end{bmatrix}$	$\mathbf{J}_1 = \begin{bmatrix} 1000 & 0 \\ 0 & 1 \end{bmatrix}$
$\mathbf{G}_1 = [g_{1,1}\ \ g_{2,1}]$	[1011.7095 270.9680]	[970.9336 248.6132]	[968.6041 248.4672]
$\mathbf{G}_2 = [g_{1,2}\ \ g_{2,2}]$	[1045.3808 285.8088]	[1214.4271 344.2183]	[1244.9045 351.8296]
$\mathbf{G}_3 = [g_{1,3}\ \ g_{2,3}]$	[969.5432 237.8358]	[1065.2226 246.5311]	[1064.6276 246.7679]
$\mathbf{G}_4 = [g_{1,4}\ \ g_{2,4}]$	[977.0561 240.2959]	[1258.9670 302.3806]	[1291.0232 309.8554]

TABLE II
VALUES OF THE CONNECTION WEIGHT AND BIAS, $m_{j,i}$ AND b_j, RESPECTIVELY, BEFORE AND AFTER THE GA PROCESS WITH $\mathbf{J}_2 = \begin{bmatrix} 0 \\ 0 \end{bmatrix}$ AND $\mathbf{J}_3 = 0.01$

Parameter	Initial parameter values	Parameter values after GA process with $\mathbf{J}_1 = \begin{bmatrix} 10 & 0 \\ 0 & 1 \end{bmatrix}$	Parameter values after GA process with $\mathbf{J}_1 = \begin{bmatrix} 100 & 0 \\ 0 & 1 \end{bmatrix}$	Parameter values after GA process with $\mathbf{J}_1 = \begin{bmatrix} 1000 & 0 \\ 0 & 1 \end{bmatrix}$
$m_{1,1}$	−0.0591	0.7778	−0.8077	−0.9895
$m_{1,2}$	0.5511	0.7389	−0.2970	−0.9875
b_1	−0.2765	−0.3715	−0.9939	−0.8823
$m_{2,1}$	−0.9863	0.9878	0.4260	0.9883
$m_{2,2}$	0.5118	0.1229	−0.2197	0.6988
b_2	−0.3234	−0.4246	−0.3110	0.8988
$m_{3,1}$	0.3058	0.1294	−0.3354	0.8199
$m_{3,2}$	0.1582	−0.8035	0.4371	0.5447
b_3	−0.7899	0.3074	0.3659	0.9925
$m_{4,1}$	−0.6254	0.2307	−0.3277	0.9690
$m_{4,2}$	−0.7569	0.0289	−0.1210	0.9922
b_4	0.4423	−0.9144	−0.7899	−0.9890

Step 5) The parameters $m_{j,i}$ and b_j of the activation function can be obtained by optimizing the performance index of (11) using the improved GA in [21] under $m_c = 2$ kg and $M_p = 30$ kg. The same $\mathbf{J}_1$, $\mathbf{J}_2$, and $\mathbf{J}_3$ are employed in the GA process. In this application example, the tunable parameters $m_{j,i}$ and b_j, $i = 1, 2;\ j = 1, 2, 3, 4$, form the chromosomes of the GA process. Their initial values are randomly generated with the minimum and maximum bounds chosen to be -1 and 1, respectively. The control parameters of the training weight w and probability of acceptance p_a of the improved GA are chosen to be 0.5 and 0.1, respectively. The population size and the number of iteration are chosen to be 10 and 200, respectively. The values of the connection weights and bias, $m_{j,i}$ and b_j, respectively, before and after the GA process are listed in Table II.

The designed sampled-data TLFCFFNN-based controller is employed to control the inverted pendulum of (12). Under the initial state conditions of $\mathbf{x}(0) = [\pi/6\ \ 0]^{\mathrm{T}}$ and $\mathbf{x}(0) = [\pi/3\ \ 0]^{\mathrm{T}}$, the system responses and control signals of the sampled-data TLFCFFNN-based control systems with $m_p = 2$ kg and $M_c = 30$ kg are shown in Fig. 3. Referring to this figure, it can be seen that the proposed sampled-data TLFCFFNN-based controller is able to stabilize the inverted pendulum. Under the same $\mathbf{J}_2$ and $\mathbf{J}_3$, $\mathbf{J}_1 = \begin{bmatrix} 100 & 0 \\ 0 & 1 \end{bmatrix}$ and $\mathbf{J}_1 = \begin{bmatrix} 1000 & 0 \\ 0 & 1 \end{bmatrix}$ are also employed to obtained other sets of

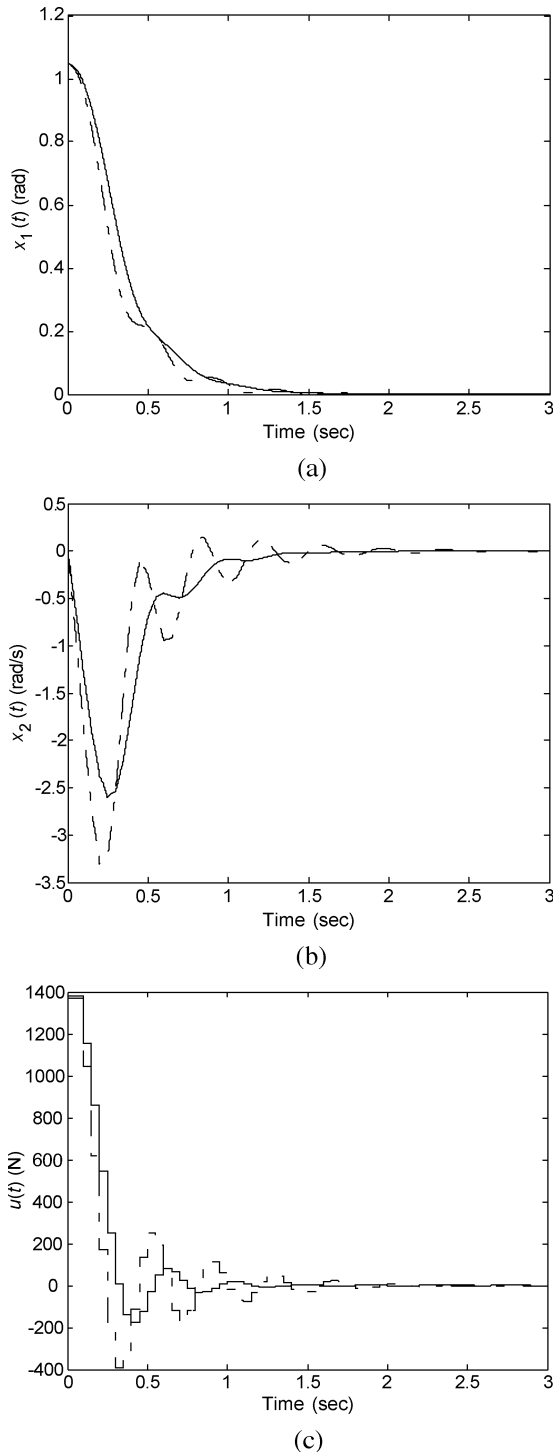

Fig. 3. System responses and control signals of the inverted pendulum with the optimized sampled-data TLFCFFNN-based controller with $h = 0.05$ s for $\mathbf{J}_1 = \begin{bmatrix} 10 & 0 \\ 0 & 1 \end{bmatrix}$ (solid lines), $\mathbf{J}_1 = \begin{bmatrix} 100 & 0 \\ 0 & 1 \end{bmatrix}$ (dotted lines), and $\mathbf{J}_1 = \begin{bmatrix} 1000 & 0 \\ 0 & 1 \end{bmatrix}$ (dashed lines), under $m_p = 2$ kg and $M_c = 30$ kg. (a) $x_1(t)$. (b) $x_2(t)$. (c) $u(t)$.

G_j as shown in Table I. It can be seen that different $\mathbf{J}_1$ place different weightings on the system states. The system responses and control signals of the sampled-data TLFCFFNN-based control systems with different $\mathbf{J}_1$ under $m_p = 2$ kg and $M_c = 30$ kg are also shown in Fig. 3. Referring to this figure, it can be seen that the optimized sampled-data TLFCFFNN-based

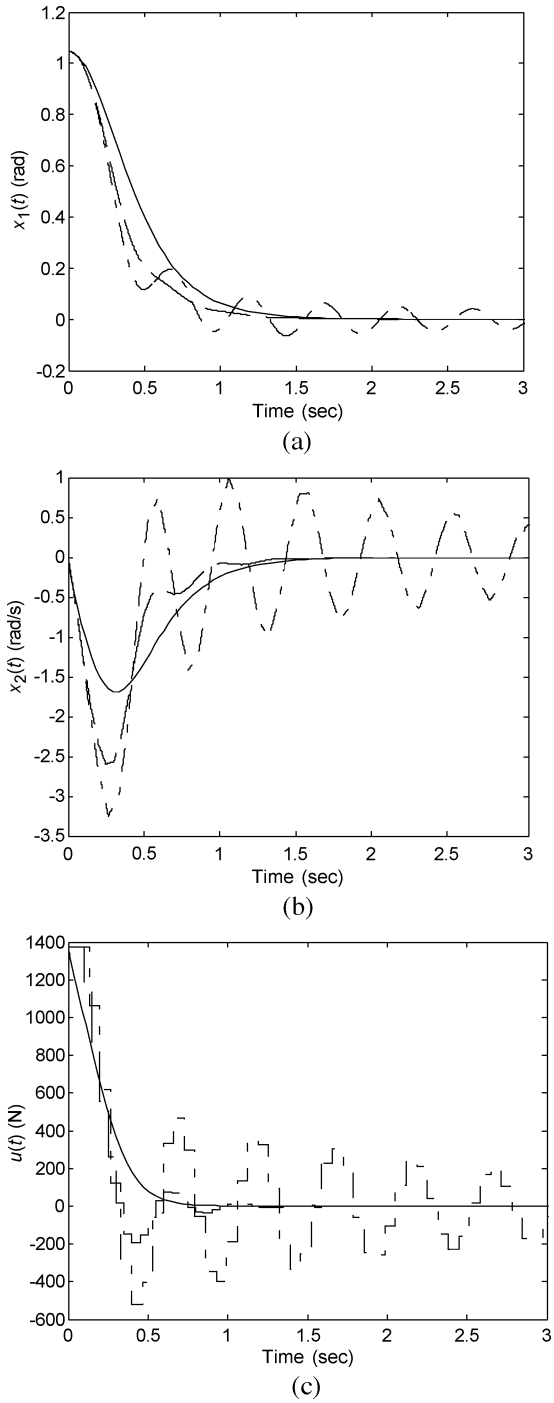

Fig. 4. System responses and control signals of the inverted pendulum with sampled-data TLFCFFNN-based controllers for $h = 0.05$ s (dashed lines), $h = h_{\max}/2$ (dotted lines), $h = h_{\max}$ (dashed–dotted lines), and the continuous-time (solid lines) with $\mathbf{J}_1 = \begin{bmatrix} 10 & 0 \\ 0 & 1 \end{bmatrix}$, $\mathbf{J}_2 = \begin{bmatrix} 0 \\ 0 \end{bmatrix}$, and $\mathbf{J}_3 = 0.01$ under $m_p = 2$ kg and $M_c = 30$ kg. (a) $x_1(t)$. (b) $x_2(t)$. (c) $u(t)$ of the TLFCFFNN-based controllers.

controller with $\mathbf{J}_1 = \begin{bmatrix} 1000 & 0 \\ 0 & 1 \end{bmatrix}$ provides the fastest transient responses, whereas that with $\mathbf{J}_1 = \begin{bmatrix} 10 & 0 \\ 0 & 1 \end{bmatrix}$ provides the slowest transient responses. Fig. 4 shows the system responses and control signals of the sampled-data TLFCFFNN-based control systems using $h = 0.05$ s, $h = h_{\max}/2$, and $h = h_{\max}$ with $\mathbf{J}_1 = \begin{bmatrix} 10 & 0 \\ 0 & 1 \end{bmatrix}$, $\mathbf{J}_2 = \begin{bmatrix} 0 \\ 0 \end{bmatrix}$, and $\mathbf{J}_3 = 0.01$, $m_p = 2$ kg and $M_c = 30$ kg. Furthermore, it can be seen that the sampled-data TLFCFFNN-based controllers using $h = h_{\max}/2$ and $h = h_{\max}$ can also stabilize the nonlinear plant.

For comparison purpose, a continuous-time TLFCFFNN-based controller of control law shown as follows is also employed to control the inverted pendulum:

$$u(t) = \sum_{j=1}^{4} m_j\left(\mathbf{x}(t)\right)\mathbf{G}_j\mathbf{x}(t). \tag{15}$$

The control signal of (15) depends on the current system states. Fig. 4 shows the system responses and control signals of the continuous-time TLFCFFNN-based control systems with $m_p = 2$ kg and $M_c = 30$ kg. The connection weights corresponding to $\mathbf{J}_1 = \begin{bmatrix} 10 & 0 \\ 0 & 1 \end{bmatrix}$ are employed in this simulation. Referring to Fig. 4, it can be seen that the sampled-data and the continuous-time TLFCFFNN-based control systems provide similar system responses and control signals. Hence, the continuous-time TLFCFFNN-based controller can be replaced by the sampled-data one. Furthermore, it is observed that a smaller sampling period of the sampled-data TLFCFFNN-based controller provides system responses closer to those of the continuous-time TLFCFFNN-based controller.

V. Conclusion

A sampled-data TLFCFFNN-based controller, which is formed by a sampler, a TLFCFFNN, and a ZOH unit, has been proposed for continuous-time nonlinear systems. Based on the Lyapunov-based approach, the stability of the sampled-data TLFCFFNN-based control systems has been investigated. Stability conditions have been derived to guarantee the system stability. The findings of the maximum value of the sampling period and the values of the network connection weights and the optimization of system performance have been formulated as generalized eigenvalue and GA minimization problems, respectively. An application example on stabilizing an inverted pendulum subject to parameter uncertainties has been given to illustrate the design procedure and the effectiveness of the proposed approach.

Appendix A

The proof of Theorem 1 will be given as follows. Based on the transformation method given in [13], the sampled-data TLFCFFNN-based control system of (9) can be written in the descriptor form, as in (A1) and (A2), shown at the bottom of the next page.

Considering (A2), we have the following property that will be used during the analysis:

$$\sum_{i=1}^{p}\sum_{j=1}^{n_h} w_i m_j \begin{bmatrix} \mathbf{0} & \mathbf{0} \\ \mathbf{A}_i + \mathbf{B}_i\mathbf{G}_j & -\mathbf{I} \end{bmatrix} \begin{bmatrix} \mathbf{x}(t) \\ \mathbf{y}(t) \end{bmatrix} - \sum_{i=1}^{p}\sum_{j=1}^{n_h} w_i m_j \begin{bmatrix} \mathbf{0} \\ \mathbf{B}_i\mathbf{G}_j \end{bmatrix} \int_{t-\tau(t)}^{t} \mathbf{y}(\varphi)d\varphi = \begin{bmatrix} \mathbf{0} \\ \mathbf{0} \end{bmatrix}. \tag{A3}$$

To investigate the system stability of the sampled-data TLFCFFNN-based control system of (9), the following Lyapunov function candidate is considered:

$$V(t) = V_1(t) + V_2(t) + V_3(t) \tag{A4}$$

where

$$V_1(t) = \mathbf{x}(t)^{\mathrm{T}}\mathbf{P}_1\mathbf{x}(t) \tag{A5}$$

$$V_2(t) = \int_{-h}^{0}\int_{t+\sigma}^{t} \mathbf{y}(\varphi)^{\mathrm{T}}\mathbf{R}\mathbf{y}(\varphi)d\varphi\, d\sigma \tag{A6}$$

$$V_3(t) = h\int_{-h}^{t} \mathbf{x}(\varphi)^{\mathrm{T}}\mathbf{S}\mathbf{x}(\varphi)d\varphi \tag{A7}$$

where $\mathbf{P}_1$, $\mathbf{R}$, and $\mathbf{S} \in \Re^{n\times n}$ are symmetric positive definite matrices. It will be shown that $\dot{V}(t) \le 0$ (equality holds when $\mathbf{x}(t) = \mathbf{y}(t) = 0$), which implies the system stability. From (A1)–(A3), (A5), and with the property that $\sum_{i=1}^{p} w_i = \sum_{j=1}^{n_h} m_j = \sum_{i=1}^{p}\sum_{j=1}^{n_h} w_i m_j = 1$, we have

$$\begin{aligned}
\dot{V}_1(t) &= \dot{\mathbf{x}}(t)^{\mathrm{T}}\mathbf{P}_1\mathbf{x}(t) + \mathbf{x}(t)^{\mathrm{T}}\mathbf{P}_1\dot{\mathbf{x}}(t) \\
&= \sum_{i=1}^{p}\sum_{j=1}^{n_h} w_i m_j \begin{bmatrix}\mathbf{x}(t)\\ \mathbf{y}(t)\end{bmatrix}^{\mathrm{T}} \\
&\quad\times\left(\mathbf{P}^{\mathrm{T}}\begin{bmatrix}\mathbf{0} & \mathbf{I}\\ \mathbf{A}_i+\mathbf{B}_i\mathbf{G}_j & -\mathbf{I}\end{bmatrix}\right. \\
&\qquad\left. + \begin{bmatrix}\mathbf{0} & (\mathbf{A}_i+\mathbf{B}_i\mathbf{G}_j)^{\mathrm{T}}\\ \mathbf{I} & -\mathbf{I}\end{bmatrix}\mathbf{P}\right)\begin{bmatrix}\mathbf{x}(t)\\ \mathbf{y}(t)\end{bmatrix} \\
&\quad - 2\sum_{i=1}^{p}\sum_{j=1}^{n_h} w_i m_j \begin{bmatrix}\mathbf{x}(t)\\ \mathbf{y}(t)\end{bmatrix}^{\mathrm{T}}\mathbf{P}^{\mathrm{T}}\begin{bmatrix}\mathbf{0}\\ \mathbf{B}_i\mathbf{G}_j\end{bmatrix}\int_{t-\tau(t)}^{t}\mathbf{y}(\varphi)d\varphi
\end{aligned} \tag{A8}$$

where $\mathbf{P} = \begin{bmatrix}\mathbf{P}_1 & \mathbf{0}\\ \mathbf{P}_2 & \mathbf{P}_3\end{bmatrix} \in \Re^{2n\times 2n}$, $\mathbf{P}_2 \in \Re^{n\times n}$, and $\mathbf{P}_3 \in \Re^{n\times n}$. From [14], based on the property that

$$\begin{aligned}
&-2\mathbf{y}(\varphi)^{\mathrm{T}}\mathbf{N}_{ij}^{\mathrm{T}}\mathbf{a}(t) \\
&\quad = -2\mathbf{a}(t)^{\mathrm{T}}\mathbf{N}_{ij}\mathbf{y}(\varphi) \\
&\quad \le \begin{bmatrix}\mathbf{y}(\varphi)\\ \mathbf{a}(t)\end{bmatrix}^{\mathrm{T}}\begin{bmatrix}\mathbf{R} & \mathbf{Y}_{ij}^{\mathrm{T}}-\mathbf{N}_{ij}^{\mathrm{T}}\\ \mathbf{Y}_{ij}-\mathbf{N}_{ij} & \mathbf{R}_{ij}\end{bmatrix}\begin{bmatrix}\mathbf{y}(\varphi)\\ \mathbf{a}(t)\end{bmatrix}
\end{aligned}$$

where

$$\begin{aligned}
&\mathbf{a}(t) = \begin{bmatrix}\mathbf{x}(t)\\ \mathbf{y}(t)\end{bmatrix} \\
&\mathbf{N}_{ij} = \mathbf{Y}_{ij} = \mathbf{P}^{\mathrm{T}}\begin{bmatrix}\mathbf{0}\\ \mathbf{B}_i\mathbf{G}_j\end{bmatrix} \\
&\mathbf{R}_{ij} = \mathbf{R}_{ij}^{\mathrm{T}} = \begin{bmatrix}\mathbf{R}_{ij}^{(11)} & \mathbf{R}_{ij}^{(21)^{\mathrm{T}}}\\ \mathbf{R}_{ij}^{(21)} & \mathbf{R}_{ij}^{(22)}\end{bmatrix} \in \Re^{2n\times 2n} \\
&\mathbf{R}_{ij}^{(11)} = \mathbf{R}_{ij}^{(11)^{\mathrm{T}}} \in \Re^{n\times n}\mathbf{R}_{ij}^{(21)} \in \Re^{n\times n} \\
&\mathbf{R}_{ij}^{(22)} = \mathbf{R}_{ij}^{(22)^{\mathrm{T}}} \in \Re^{n\times n} \\
&\begin{bmatrix}\mathbf{R} & \mathbf{Y}_{ij}^{\mathrm{T}}\\ \mathbf{Y}_{ij} & \mathbf{R}_{ij}\end{bmatrix} \ge 0, \text{ and } 0 < \tau(t) \le h
\end{aligned}$$

we have

$$\begin{aligned}
\dot{V}_1(t) &\le \sum_{i=1}^{p}\sum_{j=1}^{n_h} w_i m_j \begin{bmatrix}\mathbf{x}(t)\\ \mathbf{y}(t)\end{bmatrix}^{\mathrm{T}} \\
&\quad\times\left(\mathbf{P}^{\mathrm{T}}\begin{bmatrix}\mathbf{0} & \mathbf{I}\\ \mathbf{A}_i+\mathbf{B}_i\mathbf{G}_j & -\mathbf{I}\end{bmatrix}\right. \\
&\qquad\left. + \begin{bmatrix}\mathbf{0} & (\mathbf{A}_i+\mathbf{B}_i\mathbf{G}_j)^{\mathrm{T}}\\ \mathbf{I} & -\mathbf{I}\end{bmatrix}\mathbf{P}\right)\begin{bmatrix}\mathbf{x}(t)\\ \mathbf{y}(t)\end{bmatrix} \\
&\quad + \sum_{i=1}^{p}\sum_{j=1}^{n_h} w_i m_j \int_{t-\tau(t)}^{t}\begin{bmatrix}\mathbf{x}(t)\\ \mathbf{y}(t)\end{bmatrix}^{\mathrm{T}}\mathbf{R}_{ij}\begin{bmatrix}\mathbf{x}(t)\\ \mathbf{y}(t)\end{bmatrix}ds \\
&\quad + \sum_{i=1}^{p}\sum_{j=1}^{n_h} w_i m_j \int_{t-\tau(t)}^{t}\mathbf{y}(\varphi)^{\mathrm{T}}\mathbf{R}\mathbf{y}(\varphi)d\varphi \\
&\le \sum_{i=1}^{p}\sum_{j=1}^{n_h} w_i m_j \begin{bmatrix}\mathbf{x}(t)\\ \mathbf{y}(t)\end{bmatrix}^{\mathrm{T}} \\
&\quad\times\left(\mathbf{P}^{\mathrm{T}}\begin{bmatrix}\mathbf{0} & \mathbf{I}\\ \mathbf{A}_i+\mathbf{B}_i\mathbf{G}_j & -\mathbf{I}\end{bmatrix}\right. \\
&\qquad\left. + \begin{bmatrix}\mathbf{0} & (\mathbf{A}_i+\mathbf{B}_i\mathbf{G}_j)^{\mathrm{T}}\\ \mathbf{I} & -\mathbf{I}\end{bmatrix}\mathbf{P} + h\mathbf{R}_{ij}\right)\begin{bmatrix}\mathbf{x}(t)\\ \mathbf{y}(t)\end{bmatrix} \\
&\quad + \int_{t-\tau(t)}^{t}\mathbf{y}(\varphi)^{\mathrm{T}}\mathbf{R}\mathbf{y}(\varphi)d\varphi.
\end{aligned} \tag{A9}$$

$$\dot{\mathbf{x}}(t) = \mathbf{y}(t) \tag{A1}$$

$$\mathbf{y}(t) = \begin{cases}\sum_{i=1}^{p}\sum_{j=1}^{n_h} w_i m_j\left(\mathbf{A}_i\mathbf{x}(t) + \mathbf{B}_i\mathbf{G}_j\mathbf{x}\left(t-\tau(t)\right)\right), & \text{if } t\in[0 \quad h) \\ \sum_{i=1}^{p}\sum_{j=1}^{n_h} w_i m_j\left(\mathbf{A}_i+\mathbf{B}_i\mathbf{G}_j\right)\mathbf{x}(t) - \sum_{i=1}^{p}\sum_{j=1}^{n_h} w_i m_j\mathbf{B}_i\mathbf{G}_j\int_{t-\tau(t)}^{t}\mathbf{y}(\varphi)d\varphi, & \text{if } t\ge h\end{cases} \tag{A2}$$

From (A1)–(A3), and (A6) we have

$$\dot{V}_2(t) = h\mathbf{y}(t)^{\mathrm{T}}\mathbf{R}\mathbf{y}(t) - \int_{t-h}^{t} \mathbf{y}(\varphi)^{\mathrm{T}}\mathbf{R}\mathbf{y}(\varphi)d\varphi$$
$$= \begin{bmatrix}\mathbf{x}(t)\\ \mathbf{y}(t)\end{bmatrix}^{\mathrm{T}} \begin{bmatrix}\mathbf{0} & \mathbf{0}\\ \mathbf{0} & h\mathbf{R}\end{bmatrix} \begin{bmatrix}\mathbf{x}(t)\\ \mathbf{y}(t)\end{bmatrix} - \int_{t-h}^{t} \mathbf{y}(\varphi)^{\mathrm{T}}\mathbf{R}\mathbf{y}(\varphi)d\varphi. \tag{A10}$$

From (A1)–(A3), and (A7), we have

$$\dot{V}_3(t) = h\mathbf{x}(t)^{\mathrm{T}}\mathbf{S}\mathbf{x}(t) = \begin{bmatrix}\mathbf{x}(t)\\ \mathbf{y}(t)\end{bmatrix}^{\mathrm{T}} \begin{bmatrix}h\mathbf{S} & \mathbf{0}\\ \mathbf{0} & \mathbf{0}\end{bmatrix} \begin{bmatrix}\mathbf{x}(t)\\ \mathbf{y}(t)\end{bmatrix}. \tag{A11}$$

From (A9)–(A11) and with the fact that $\int_{t-h}^{t} \mathbf{y}(\varphi)^{\mathrm{T}}\mathbf{R}\mathbf{y} \times (\varphi)d\varphi \geq \int_{t-\tau(t)}^{t} \mathbf{y}(\varphi)^{\mathrm{T}}\mathbf{R}\mathbf{y}(\varphi)d\varphi$ subject to $0 < \tau(t) \leq h$ and $\mathbf{R} > 0$, we have

$$\dot{V}(t) \leq \sum_{i=1}^{p}\sum_{j=1}^{n_h} w_i m_j \begin{bmatrix}\mathbf{x}(t)\\ \mathbf{y}(t)\end{bmatrix}^{\mathrm{T}} \mathbf{Q}_{ij} \begin{bmatrix}\mathbf{x}(t)\\ \mathbf{y}(t)\end{bmatrix} \tag{A12}$$

where

$$\mathbf{Q}_{ij} = \mathbf{P}^{\mathrm{T}} \begin{bmatrix}\mathbf{0} & \mathbf{I}\\ \mathbf{A}_i + \mathbf{B}_i\mathbf{G}_j & -\mathbf{I}\end{bmatrix} + \begin{bmatrix}\mathbf{0} & (\mathbf{A}_i + \mathbf{B}_i\mathbf{G}_j)^{\mathrm{T}}\\ \mathbf{I} & -\mathbf{I}\end{bmatrix} \mathbf{P} + h\mathbf{R}_{ij} + \begin{bmatrix}h\mathbf{S} & \mathbf{0}\\ \mathbf{0} & h\mathbf{R}\end{bmatrix}. \tag{A13}$$

It can be seen that $\dot{V}(t) \leq 0$ (equality holds when $\mathbf{x}(t) = \mathbf{y}(t) = 0$) if $\mathbf{Q}_{ij} < 0$ and $\begin{bmatrix}\mathbf{R} & \mathbf{Y}_{ij}^{\mathrm{T}}\\ \mathbf{Y}_{ij} & \mathbf{R}_{ij}\end{bmatrix} \geq 0$ for all i and j. This implies that the sampled-data TLFCFFNN-based control system is asymptotically stable, i.e., $\mathbf{x}(t) \to 0$ as $t \to \infty$. Let

$$\mathbf{X} = \begin{bmatrix}\mathbf{X}_1 & \mathbf{0}\\ \mathbf{X}_2 & \mathbf{X}_3\end{bmatrix} = \mathbf{P}^{-1}$$

where $\mathbf{X}_1 = \mathbf{X}_1^{\mathrm{T}}$, $\mathbf{G}_j = \mathbf{N}_j\mathbf{X}_1^{-1}$, and

$$\mathbf{X}^{\mathrm{T}}\mathbf{R}_{ij}\mathbf{X} = \mathbf{M}_{ij} = \mathbf{M}_{ij}^{\mathrm{T}} = \begin{bmatrix}\mathbf{M}_{ij}^{(11)} & \mathbf{M}_{ij}^{(21)^{\mathrm{T}}}\\ \mathbf{M}_{ij}^{(21)} & \mathbf{M}_{ij}^{(22)}\end{bmatrix} \in \Re^{2n\times 2n}$$

where $\mathbf{M}_{ij}^{(11)} = \mathbf{M}_{ij}^{(11)^{\mathrm{T}}} \in \Re^{n\times n}$, $\mathbf{M}_{ij}^{(21)} \in \Re^{n\times n}$, $\mathbf{M}_{ij}^{(22)} = \mathbf{M}_{ij}^{(22)^{\mathrm{T}}} \in \Re^{n\times n}$, $\mathbf{M} = \mathbf{R}^{-1}$, and $\mathbf{Y} = \mathbf{S}^{-1}$, from (A13), we have (A14), shown at the bottom of the page. By Schur complement, the inequality of (A14) is equivalent to the LMIs in (A15), shown at the bottom of the page. From (A13), it is required that $\begin{bmatrix}\mathbf{R} & \mathbf{Y}_{ij}^{\mathrm{T}}\\ \mathbf{Y}_{ij} & \mathbf{R}_{ij}\end{bmatrix} \geq 0$. Premultiply $\mathrm{diag}\{\mathbf{X}_1, \mathbf{X}^{\mathrm{T}}\}$ and postmultiply $\mathrm{diag}\{\mathbf{X}_1, \mathbf{X}\}$ to $\begin{bmatrix}\mathbf{R} & \mathbf{Y}_{ij}^{\mathrm{T}}\\ \mathbf{Y}_{ij} & \mathbf{R}_{ij}\end{bmatrix} \geq 0$, we have

$$\begin{bmatrix}\mathbf{X}_1 & \mathbf{0}\\ \mathbf{0} & \mathbf{X}\end{bmatrix}^{\mathrm{T}} \begin{bmatrix}\mathbf{R} & \mathbf{Y}_{ij}^{\mathrm{T}}\\ \mathbf{Y}_{ij} & \mathbf{R}_{ij}\end{bmatrix} \begin{bmatrix}\mathbf{X}_1 & \mathbf{0}\\ \mathbf{0} & \mathbf{X}\end{bmatrix} \geq 0$$
$$= \begin{bmatrix}\mathbf{X}_1\mathbf{M}^{-1}\mathbf{X}_1 & \mathbf{0} & \mathbf{N}_j^{\mathrm{T}}\mathbf{B}_i^{\mathrm{T}}\\ \mathbf{0} & \mathbf{M}_{ij}^{(11)} & \mathbf{M}_{ij}^{(21)^{\mathrm{T}}}\\ \mathbf{B}_i\mathbf{N}_j & \mathbf{M}_{ij}^{(21)} & \mathbf{M}_{ij}^{(22)}\end{bmatrix} \geq 0. \tag{A16}$$

It should be noted that (A16) is not an LMI due to the existence of the term $\mathbf{X}_1\mathbf{M}^{-1}\mathbf{X}_1$. However, based on the following property, (A16) can be represented as an LMI. With the property that $\mathbf{M} = \mathbf{M}^{\mathrm{T}}$, we consider the following inequality:

$$(\mathbf{X}_1 - \mathbf{M})^{\mathrm{T}}\mathbf{M}^{-1}(\mathbf{X}_1 - \mathbf{M}) = \mathbf{X}_1^{\mathrm{T}}\mathbf{M}^{-1}\mathbf{X}_1 - \mathbf{X}_1^{\mathrm{T}} - \mathbf{X}_1 + \mathbf{M} > 0$$
$$\Rightarrow \mathbf{X}_1\mathbf{M}^{-1}\mathbf{X}_1 > 2\mathbf{X}_1 - \mathbf{M}. \tag{A17}$$

$$\mathbf{X}^{\mathrm{T}}\left(\mathbf{P}^{\mathrm{T}}\begin{bmatrix}\mathbf{0} & \mathbf{I}\\ \mathbf{A}_i + \mathbf{B}_i\mathbf{G}_j & -\mathbf{I}\end{bmatrix} + \begin{bmatrix}\mathbf{0} & (\mathbf{A}_i + \mathbf{B}_i\mathbf{G}_j)^{\mathrm{T}}\\ \mathbf{I} & -\mathbf{I}\end{bmatrix}\mathbf{P} + h\mathbf{R}_{ij} + \begin{bmatrix}h\mathbf{S} & \mathbf{0}\\ \mathbf{0} & h\mathbf{R}\end{bmatrix}\right)\mathbf{X} < 0$$
$$= \begin{bmatrix}\mathbf{0} & \mathbf{I}\\ \mathbf{A}_i + \mathbf{B}_i\mathbf{G}_j & -\mathbf{I}\end{bmatrix}\begin{bmatrix}\mathbf{X}_1 & \mathbf{0}\\ \mathbf{X}_2 & \mathbf{X}_3\end{bmatrix} + \begin{bmatrix}\mathbf{X}_1 & \mathbf{X}_2^{\mathrm{T}}\\ \mathbf{0} & \mathbf{X}_3^{\mathrm{T}}\end{bmatrix}\begin{bmatrix}\mathbf{0} & (\mathbf{A}_i + \mathbf{B}_i\mathbf{G}_j)^{\mathrm{T}}\\ \mathbf{I} & -\mathbf{I}\end{bmatrix} + h\mathbf{X}^{\mathrm{T}}\mathbf{R}_{ij}\mathbf{X} + \mathbf{X}^{\mathrm{T}}\begin{bmatrix}h\mathbf{S} & \mathbf{0}\\ \mathbf{0} & h\mathbf{R}\end{bmatrix}\mathbf{X} < 0$$
$$= \begin{bmatrix}\mathbf{X}_2 + \mathbf{X}_2^{\mathrm{T}} + h\mathbf{M}_{ij}^{(11)} & \mathbf{X}_1\mathbf{A}_i^{\mathrm{T}} + \mathbf{N}_j^{\mathrm{T}}\mathbf{B}_i^{\mathrm{T}} - \mathbf{X}_2^{\mathrm{T}} + \mathbf{X}_3 + h\mathbf{M}_{ij}^{(21)^{\mathrm{T}}}\\ \mathbf{A}_i\mathbf{X}_1 + \mathbf{B}_i\mathbf{N}_j - \mathbf{X}_2 + \mathbf{X}_3^{\mathrm{T}} + h\mathbf{M}_{ij}^{(21)} & -\mathbf{X}_3 - \mathbf{X}_3^{\mathrm{T}} + h\mathbf{M}_{ij}^{(22)}\end{bmatrix} + \mathbf{X}^{\mathrm{T}}\begin{bmatrix}h\mathbf{S} & \mathbf{0}\\ \mathbf{0} & h\mathbf{R}\end{bmatrix}\mathbf{X} < 0 \tag{A14}$$

$$\begin{bmatrix}\mathbf{X}_2 + \mathbf{X}_2^{\mathrm{T}} + h\mathbf{M}_{ij}^{(11)} & \mathbf{X}_1\mathbf{A}_i^{\mathrm{T}} + \mathbf{N}_j^{\mathrm{T}}\mathbf{B}_i^{\mathrm{T}} - \mathbf{X}_2^{\mathrm{T}} + \mathbf{X}_3 + h\mathbf{M}_{ij}^{(21)^{\mathrm{T}}} & h\mathbf{X}_1 & h\mathbf{X}_2^{\mathrm{T}}\\ \mathbf{A}_i\mathbf{X}_1 + \mathbf{B}_i\mathbf{N}_j - \mathbf{X}_2 + \mathbf{X}_3^{\mathrm{T}} + h\mathbf{M}_{ij}^{(21)} & -\mathbf{X}_3 - \mathbf{X}_3^{\mathrm{T}} + h\mathbf{M}_{ij}^{(22)} & \mathbf{0} & h\mathbf{X}_3^{\mathrm{T}}\\ h\mathbf{X}_1 & \mathbf{0} & -h\mathbf{Y} & \mathbf{0}\\ h\mathbf{X}_2 & h\mathbf{X}_3 & \mathbf{0} & -h\mathbf{M}\end{bmatrix} < 0,$$
$$i = 1, 2, \ldots, p; \quad j = 1, 2, \ldots, n_h \tag{A15}$$

From (A16) and (A17), it can be seen that the holding of the following LMIs implies the holding of (A16):

$$\begin{bmatrix} 2\mathbf{X}_1 - \mathbf{M} & \mathbf{0} & \mathbf{N}_j^{\mathrm{T}}\mathbf{B}_i^{\mathrm{T}} \\ \mathbf{0} & \mathbf{M}_{ij}^{(11)} & \mathbf{M}_{ij}^{(21)^{\mathrm{T}}} \\ \mathbf{B}_i\mathbf{N}_j & \mathbf{M}_{ij}^{(21)} & \mathbf{M}_{ij}^{(22)} \end{bmatrix} \geq 0, \quad i = 1, 2, \ldots, p,\ j = 1, 2, \ldots, n_h. \tag{A18}$$

The sampled-data TLFCFFNN-based control system of (9) is guaranteed to be stable if the LMIs of (A15) and (A18) are satisfied. The largest sampling period can be obtained by maximizing the value of h subject to the stability conditions of (A15) and (A18). ■

APPENDIX B

The proof of Theorem 2 will be given as follows. From (6) and (10), we have

$$\begin{aligned} J &= \int_{\tau_0}^{\tau_1} \left[\mathbf{x}(t_\gamma)^{\mathrm{T}} \left(\sum_{j=1}^{n_h} m_j \mathbf{G}_j \mathbf{x}(t_\gamma) \right)^{\mathrm{T}} \right] \\ &\quad \times \begin{bmatrix} \mathbf{J}_1 & \mathbf{J}_2 \\ \mathbf{J}_2^{\mathrm{T}} & \mathbf{J}_3 \end{bmatrix} \begin{bmatrix} \mathbf{x}(t_\gamma) \\ \sum_{l=1}^{n_h} m_l \mathbf{G}_l \mathbf{x}(t_\gamma) \end{bmatrix} dt_\gamma \\ &= \int_{\tau_0}^{\tau_1} \sum_{j=1}^{n_h} \sum_{l=1}^{n_h} m_j m_l \mathbf{x}(t_\gamma)^{\mathrm{T}} \\ &\quad \times \left(\mathbf{J}_1 + \mathbf{G}_j^{\mathrm{T}}\mathbf{J}_2^{\mathrm{T}} + \mathbf{J}_2\mathbf{G}_l + \mathbf{G}_j^{\mathrm{T}}\mathbf{J}_3\mathbf{G}_l \right) \mathbf{x}(t_\gamma) dt_\gamma. \end{aligned} \tag{B1}$$

The system performance can be optimized by minimizing the performance index J. Let $J < \eta \int_{\tau_0}^{\tau_1} \mathbf{x}(t_\gamma)^{\mathrm{T}} \mathbf{X}_1^{-1} \mathbf{X}_1^{-1} \mathbf{x}(t_\gamma) dt_\gamma$, where η is a nonzero positive scalar. By minimizing the value of η, the performance index J can be minimized. Hence, from (B1), we have

$$\begin{aligned} \int_{t_o}^{t_1} \sum_{j=1}^{n_h} \sum_{j=1}^{n_h} m_j m_l \mathbf{x}(t_\gamma)^{\mathrm{T}} \mathbf{X}_1^{-1} \left(\mathbf{X}_1\mathbf{J}_1\mathbf{X}_1 + \mathbf{X}_1\mathbf{G}_j^{\mathrm{T}}\mathbf{J}_2^{\mathrm{T}}\mathbf{X}_1 \right. \\ \left. + \mathbf{X}_1\mathbf{J}_2\mathbf{G}_j\mathbf{X}_1 + \mathbf{X}_1\mathbf{G}_j^{\mathrm{T}}\mathbf{J}_3\mathbf{G}_l\mathbf{X}_1 - \eta\mathbf{I} \right) \mathbf{X}_1^{-1}\mathbf{x}(t_\gamma)\, dt_\gamma < 0. \end{aligned} \tag{B2}$$

From (B2) and let $\mathbf{G}_j = \mathbf{N}_j\mathbf{X}_1^{-1}$, we have

$$\begin{aligned} \int_{\tau_0}^{\tau_1} \sum_{j=1}^{n_h} \sum_{j=1}^{n_h} m_j m_l \mathbf{x}(t_\gamma)^{\mathrm{T}} \mathbf{X}_1^{-1} \left(\mathbf{X}_1\mathbf{J}_1\mathbf{X}_1 + \mathbf{N}_j^{\mathrm{T}}\mathbf{J}_2^{\mathrm{T}}\mathbf{X}_1 \right. \\ \left. + \mathbf{X}_1\mathbf{J}_2\mathbf{N}_j + \mathbf{N}_j^{\mathrm{T}}\mathbf{J}_3\mathbf{N}_l - \eta\mathbf{I} \right) \mathbf{X}_1^{-1}\mathbf{x}(t_\gamma) dt_\gamma < 0. \end{aligned} \tag{B3}$$

Based on the facts that $\mathbf{J}_3 > 0$ and $(\mathbf{N}_j - \mathbf{N}_l)^{\mathrm{T}}\mathbf{J}_3(\mathbf{N}_j - \mathbf{N}_l) \geq 0$, we have $\mathbf{N}_j^{\mathrm{T}}\mathbf{J}_3\mathbf{N}_j \geq \mathbf{N}_j^{\mathrm{T}}\mathbf{J}_3\mathbf{N}_l$. The holding of the following inequality implies the holding of (B3):

$$\begin{aligned} \int_{t_o}^{t_1} \sum_{j=1}^{n_h} m_j \mathbf{x}(t_\gamma)^{\mathrm{T}} \mathbf{X}_1^{-1} \left(\mathbf{X}_1\mathbf{J}_1\mathbf{X}_1 + \mathbf{N}_j^{\mathrm{T}}\mathbf{J}_2^{\mathrm{T}}\mathbf{X}_1 + \mathbf{X}_1\mathbf{J}_2\mathbf{N}_j \right. \\ \left. + \mathbf{N}_j^{\mathrm{T}}\mathbf{J}_3\mathbf{N}_j - \eta\mathbf{I} \right) \mathbf{X}_1^{-1}\mathbf{x}(t_\gamma) dt_\gamma < 0. \end{aligned} \tag{B4}$$

It can further be seen that (B4) holds if the following inequalities holds:

$$\mathbf{X}_1\mathbf{J}_1\mathbf{X}_1 + \mathbf{N}_j^{\mathrm{T}}\mathbf{J}_2^{\mathrm{T}}\mathbf{X}_1 + \mathbf{X}_1\mathbf{J}_2\mathbf{N}_j + \mathbf{N}_j^{\mathrm{T}}\mathbf{J}_3\mathbf{N}_j - \eta\mathbf{I} < 0, \quad j = 1, 2, \ldots, n_h. \tag{B5}$$

By Schur complement, (B5) is equivalent to the following LMIs, respectively:

$$\begin{bmatrix} -\eta\mathbf{I} & \mathbf{X}_1 & \mathbf{N}_j^{\mathrm{T}} \\ \mathbf{X}_1 & -\begin{bmatrix} \mathbf{J}_1 & \mathbf{J}_2 \\ \mathbf{J}_2^{\mathrm{T}} & \mathbf{J}_3 \end{bmatrix}^{-1} \\ \mathbf{N}_j & \end{bmatrix} < 0, \qquad j = 1, 2, \ldots, n_h. \tag{B6}$$

■

APPENDIX C

The parameters of the system model of (13) are listed as follows:

$$\mathbf{A}_1 = \mathbf{A}_2 = \begin{bmatrix} 0 & 1 \\ f_{1_{\min}} & 0 \end{bmatrix} \quad \mathbf{A}_3 = \mathbf{A}_4 = \begin{bmatrix} 0 & 1 \\ f_{1_{\max}} & 0 \end{bmatrix}$$
$$\mathbf{B}_1 = \mathbf{B}_3 = \begin{bmatrix} 0 \\ f_{2_{\min}} \end{bmatrix} \quad \mathbf{B}_2 = \mathbf{B}_4 = \begin{bmatrix} 0 \\ f_{2_{\max}} \end{bmatrix}$$

where $f_{1_{\min}} = 11.3533$, $f_{1_{\max}} = 16.4640$, $f_{2_{\min}} = -0.0192$, and $f_{2_{\max}} = -0.0492$

$$w_i(\mathbf{x}(t)) = \frac{\mu_{\mathrm{M}_1^i}(f_1(\mathbf{x}(t))) \times \mu_{\mathrm{M}_2^i}(f_2(\mathbf{x}(t)))}{\sum_{l=1}^{4} \left(\mu_{\mathrm{M}_1^l}(f_1(\mathbf{x}(t))) \times \mu_{\mathrm{M}_2^l}(f_2(\mathbf{x}(t))) \right)}$$

$$\mu_{\mathrm{M}_1^\beta}(f_1(\mathbf{x}(t))) = \frac{-f_1(\mathbf{x}(t)) + f_{1_{\max}})}{f_{1_{\max}} - f_{1_{\min}}}$$

for $\beta = 1, 2$;

$$\mu_{\mathrm{M}_1^\delta}(f_1(\mathbf{x}(t))) = 1 - \mu_{\mathrm{M}_1^1}(f_1(\mathbf{x}(t)))$$

for $\delta = 3, 4$;

$$\mu_{\mathrm{M}_2^\kappa}(f_2(\mathbf{x}(t))) = \frac{-f_2(\mathbf{x}(t)) + f_{2_{\max}}}{f_{2_{\max}} - f_{2_{\min}}}$$

for $\kappa = 1, 3$ and

$$\mu_{\mathrm{M}_2^\phi}(f_2(\mathbf{x}(t))) = 1 - \mu_{\mathrm{M}_2^1}(f_2(\mathbf{x}(t)))$$

for $\phi = 2, 4$;

$$f_1(\mathbf{x}(t)) = \frac{g - am_pLx_2(t)^2 \cos(x_1(t)))}{\frac{4L}{3} - am_pL\cos^2(x_1(t))} \left(\frac{\sin(x_1(t))}{x_1(t)}\right)$$

and

$$f_2(\mathbf{x}(t)) = -\frac{a\cos(x_1(t))}{\frac{4L}{3} - am_pL\cos^2(x_1(t))}.$$

REFERENCES

[1] B. Widrow and M. A. Lehr, "30 years of adaptive neural networks: Perceptron, madaline, and backpropagation," *Proc. IEEE*, vol. 78, no. 9, pp. 1415–1442, Sep. 1990.

[2] M. Li, K. Mechrotra, C. Mohan, and S. Ranka, "Sunspot numbers forecasting using neural network," in *Proc. 5th IEEE Int. Symp. Intell. Control*, 1990, pp. 524–528.

[3] H. K. Lam and F. H. F. Leung, "Digit and command interpretation using neural network and genetic algorithm," *IEEE Trans. Syst., Man, Cybern B, Cybern.*, vol. 34, no. 6, pp. 2273–2283, Dec. 2004.

[4] F. L. Lewis, K. Liu, and A. Yesildirek, "Network net robot controller with guaranteed tracking performance," *IEEE Trans. Neural Netw.*, vol. 6, no. 3, pp. 703–715, May 1995.

[5] G. P. Liu, V. Kadirkamanathan, and S. A. Billings, "Variable neural networks for adaptive control of nonlinear systems," *IEEE Trans. Syst., Man, Cybern. C, Appl. Rev.*, vol. 29, no. 1, pp. 34–43, Feb. 1999.

[6] H. D. Patiño, R. Carelli, and B. R. Kuchen, "Neural network for advanced control of robot manipulators," *IEEE Trans. Neural Netw.*, vol. 13, no. 2, pp. 343–354, Mar. 2002.

[7] C. L. Hwang, "Neural-network-based variable structure control of electrohydraulic servosystems subject to huge uncertainties without persistent excitation," *IEEE/ASME Trans. Mechatron.*, vol. 4, no. 1, pp. 50–59, Mar. 1999.

[8] S. Lin and A. A. Goldenberg, "Neural-network control of mobile manipulators," *IEEE Trans. Neural Netw.*, vol. 12, no. 5, pp. 1121–1133, Sep. 2001.

[9] C. L. Lin, "Control of perturbed systems using neural networks," *IEEE Trans. Neural Netw.*, vol. 9, no. 5, pp. 1046–1050, Sep. 1998.

[10] K. Tanaka, "Stability and stabilizability of fuzzy-neural-linear control systems," *IEEE Trans. Fuzzy Syst.*, vol. 3, no. 4, pp. 438–447, Nov. 1995.

[11] ——, "An approach to stability criteria of neural-network control systems," *IEEE Trans. Neural Netw.*, vol. 7, no. 3, pp. 629–642, May 1996.

[12] J. D. Hwang and F. H. Hsiao, "Stability analysis of neural network interconnected systems," *IEEE Trans. Neural Netw.*, vol. 14, no. 1, pp. 201–208, Jan. 2003.

[13] E. Fridman, A. Seuret, and J. P. Richard, "Robust sampled-data stabilization of linear systems: An output delay approach," *Automatica*, vol. 40, no. 8, pp. 1441–1446, Aug. 2004.

[14] Y. S. Moon, P. Park, W. H. Kwon, and Y. S. Lee, "Delay-dependent robust stabilization of uncertain state-delayed systems," *Int. J. Control*, vol. 74, no. 14, pp. 1447–1455, Sep. 2001.

[15] E. Fridman, "Stability of linear descriptor systems with delay: A Lyapunov-based approach," *J. Math. Anal. Appl.*, vol. 273, no. 1, pp. 24–44, Sep. 2002.

[16] X. P. Guan and C. L. Chen, "Delay-dependent guaranteed cost control for T–S fuzzy systems with time delays," *IEEE Trans. Fuzzy Syst.*, vol. 12, no. 2, pp. 236–249, Apr. 2004.

[17] S. Boyd, L. El Ghaoui, E. Feron, and V. Balakrishnan, *Linear Matrix Inequalities in System and Control Theory*. Philadelphia, PA: SIAM, 1994.

[18] Z. Michalewicz, *Genetic Algorithm + Data Structures = Evolution Programs*, 2nd ed. Berlin, Germany: Springer-Verlag, 1994.

[19] F. M. Ham and I. Kostanic, *Principles of Neurocomputing for Science and Engineering*. New York: McGraw-Hill, 2001.

[20] B. D. O. Anderson and J. B. Moore, *Optimal Control: Linear Quadratic Methods*. Englewood Cliffs, NJ: Prentice-Hall, 1990.

[21] F. H. F. Leung, H. K. Lam, S. H. Ling, and P. K. S. Tam, "Tuning of the structure and parameters of neural network using an improved genetic algorithm," *IEEE Trans. Neural Netw.*, vol. 14, no. 1, pp. 79–88, Jan. 2003.

[22] E. Kim, M. Park, S. Ji, and M. Park, "A new approach to fuzzy modeling," *IEEE Trans. Fuzzy Syst.*, vol. 5, no. 3, pp. 328–337, Aug. 1997.

[23] K. Tanaka, T. Ikeda, and H. O. Wang, "Robust stabilization of a class of uncertain nonlinear systems via fuzzy control: Quadratic stability, H^∞ control theory, and linear matrix inequalities," *IEEE Trans. Fuzzy Syst.*, vol. 4, no. 1, pp. 1–13, Feb. 1996.

H. K. Lam (M'98) received the B.Eng. (Hons.) and Ph.D. degrees in electronic engineering from the Hong Kong Polytechnic University, Kowloon, in 1995 and 2000, respectively.

From 2000 to 2005, he was with the Department of Electronic and Information Engineering, Hong Kong Polytechnic University, as Postdoctoral and Research Fellows, respectively. In 2005, he joined as a Lecturer in King's College London, London, U.K. His current research interests include intelligent control and systems and computational intelligence.

Frank H. F. Leung (M'92–SM'03) was born in Hong Kong in 1964. He received the B.Eng. and Ph.D. degrees in electronic engineering from the Hong Kong Polytechnic University, Kowloon, in 1988 and 1992, respectively.

He joined the Hong Kong Polytechnic University in 1992 and is now an Associate Professor in the Department of Electronic and Information Engineering. He is active in research and has published over 130 research papers on computational intelligence, control, and power electronics. At present, he is involved in the R&D on Intelligent Multimedia Home and Powerline Communications. He has been serving as a reviewer for many international journals and has been helping the organization of many international conferences. Currently, he is an Executive Committee Member of IEEE Hong Kong Chapter of Signal Processing. He is also a Chartered Engineer and a Corporate Member of the Institution of Electrical Engineers, U.K.